JOURNAL OF MATERIALS SCIENCE 13 (1978) 1031–1037

Thermal cyclic loading in a Co-Cr-Al-C eutectic composite

U. W. HILDEBRANDT, P. R. SAHM
Brown Boveri Central Research Laboratory, Heidelberg, Germany

Thermal fatigue measurements have been carried out with aligned eutectic Co–Cr–Al–C alloys. The following were observed: (a) ripening; (b) partial carbide transformations; (c) irreversible strain effects. These effects have been evaluated qualitatively, and to explain the irreversible strain a model has been proposed in which both the differential thermal expansion between matrix and fibre and the deformation rate dependence of yield stress are considered.

1. Introduction

Structural stability is an important criterion for the application of high-temperature alloys in gas turbine blades and vanes. Structural stability essentially determines creep properties, fatigue strength, and corrosion behaviour. The structural stability is itself influenced by thermal fatigue stressing, i.e. the interactions are considerable and cannot be neglected.

Structural stability in directionally solidified eutectic superalloys is determined by the interaction between the matrix and the other (in most cases mechanically stronger and directionally aligned) phases. The following external parameters are to be considered [1]: (a) temperature $T_{\max}$ and time Δt (at $T_{\max}$ or $T_{\min}$ respectively) long term stability in an isothermal environment; (b) heating and cooling rates $\mathrm{d}T/\mathrm{d}t$ and temperature difference $\Delta T = T_{\max} - T_{\min}$; (c) thermal cyclic loading; and (d) superimposed stresses and strains.

These parameters cause temperature gradients $\Delta T/\Delta X = G$ in the sample which, in turn, affect the structural stability. Mechanical and physical properties of the sample to be investigated are also important in this consideration [1]. These are: (a) sample geometry; (b) heat conduction and radiation constants (λ and ϵ); (c) thermal expansion differences of the phases involved ($\Delta\alpha = \alpha_1 - \alpha_2$); (d) mutual solubility of the phases ($c_i = c_i(T)$); (e) interface energies of matrix and other phases σ_{Gi}; (f) structural perfection of the reinforcing phases; and (g) various transformations, e.g. phase transformations (see also solubility changes) and allotropic transformations. This report deals mainly with the ripening process of chromium carbide fibres and the irreversible strain effects observed under thermal cyclic loading in the eutectic Co, 30 Cr, 2 Al – $(\mathrm{Cr_6Co_{0.8}Al_{0.2}})\mathrm{C_3}$.

2. Experimental procedure

Thermal fatigue measurements were conducted in the apparatus shown in Fig. 1. The specimen holder was constructed in such a way that the sample was not subjected to compressive forces during the heating cycle. The effect of thermal expansion on undesirable residual forces was kept low by gripping the sample between two elastic Cu-plated electrodes (Fig. 1). Air or water was used for quenching. The samples were heated by direct current. Figs. 2 and 3 show the temperature cycle and the temperature gradient developed in the longitudinal direction (to be distinguished from the transverse gradient also present). The detailed experimental parameters were: $T_{\max} = 1000^\circ$ C, $T_{\min} = 25^\circ$ C, $G_{\text{air}} \simeq 20\,\mathrm{K\,sec^{-1}}$, $G_{\mathrm{H_2O}} \simeq 150\,\mathrm{K\,sec^{-1}}$ in the range between 1000 and 200° C (see Fig. 2).

$$\begin{aligned}\Delta t_{\text{total}} &= \Delta t_{\text{heat}} + \Delta t_{\text{cool}}\\ &= 120\,\text{sec (air)}\\ &= 60\,\text{sec}\ (\mathrm{H_2O}).\end{aligned}$$

The evaluation was based on the stability analysis of the eutectic structure, mainly by metal-

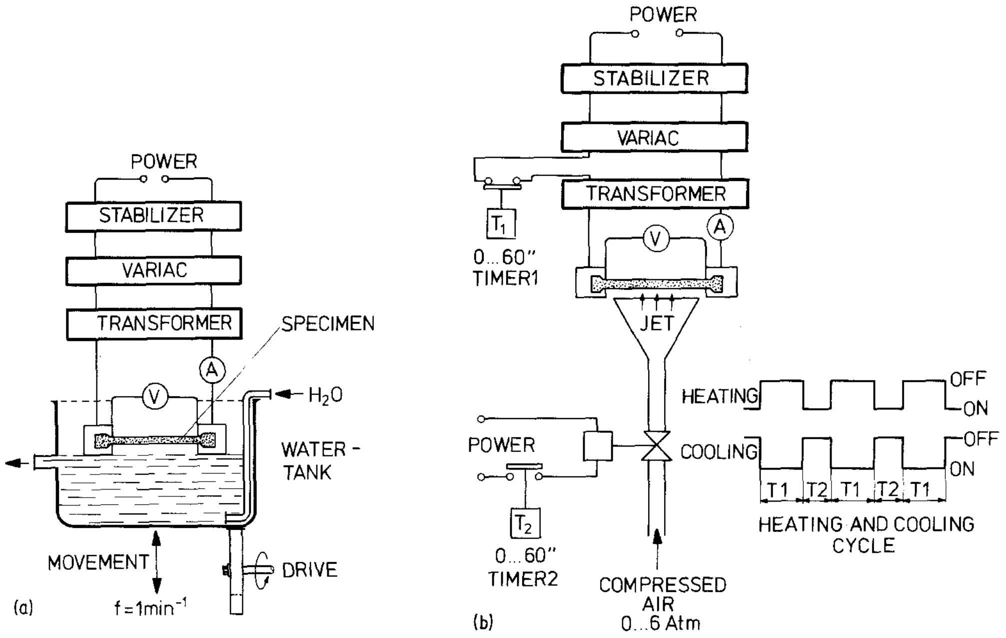

Figure 1 (a) Quenching equipment; water quenching (after Sahm *et al.* [10]). (b) Quenching equipment; air quenching.

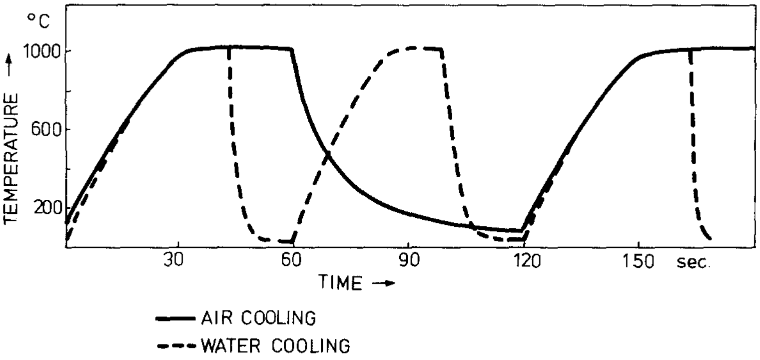

Figure 2 Quenching curves; temperatures refer to specimen centres.

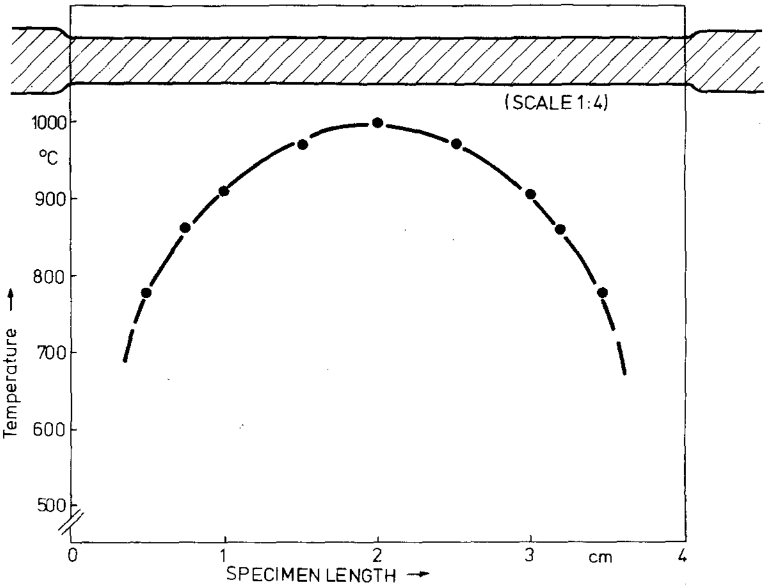

Figure 3 Temperature gradient along sample at maximum of temperature cycle.

lography (optical microscopy and microprobe analysis). Since the T-gradient had been calibrated in the longitudinal direction of the sample, it was possible to correlate the microstructural appearance with T–t history. The alloys used in this investigation were of the composition (wt%) 59.9 Co, 38.9 Cr, 2.2 C, 2.0 Al. Using pre-alloyed rods of the above composition, specimens were directionally solidified under vacuum at $5\,\mathrm{cm\,h^{-1}}$ in a temperature gradient of $200\,\mathrm{K\,cm^{-1}}$.

3. Results

3.1. Air quenching

The thermal fatigue experiments yielded the following characteristic macroscopic effects: (a) irreversible elongation of the sample; (b) constriction in the centre of the sample (for $T_{\max} >$ 900° C), and (c) formation of longitudinal grooves. Possible reasons for these phenomena are given below. Structural changes were rather obvious, and they appeared to be independent of the method of quenching.

Structural effects were two-fold; firstly, partial transformation of the K_2'-phase into K_3'

$$K_2' \rightarrow K_3'$$

$$(\mathrm{Cr_6Co_{0.8}Al_{0.2}})\mathrm{C_3^*} \rightarrow (\mathrm{Cr}_{23-(x+y)}\mathrm{Co}_x\mathrm{Al}_y)\mathrm{C}_6,$$

and secondly, the ripening process of both phases aided by both spheroidization and solubility effects.

The amount of transformed carbides appears to be constant at 5 to 10 vol%. Obviously, the fraction of transformed carbide is determined by the position of the alloy within the phase diagram. Generally it seems that the solubility line between $(\gamma + K_2' + K_3')$ and $(\gamma + K_2')$ of an Al-alloyed Co–Cr–C material shifts towards higher Co contents (see Fig. 4).

Fig. 5 shows the microstructures after 10^4 cycles. The T gradient in the sample allows the study of the above mentioned ripening processes at cycles carried out with different $T_{\max}$. Spheroidization appears to be particularly strong in transformed areas of the microstructure.

3.2. Water quenching

The following macroscopic changes of the sample are typical for water quenched samples as contrasted to the air quenched case: (a) formation of oxides in the surface layer; (b) no constriction and very little longitudinal expansion. The thickness of the oxide layer depended strongly on temperature and thus increased symmetrically towards the middle of the sample (see Fig. 2). Ripening and

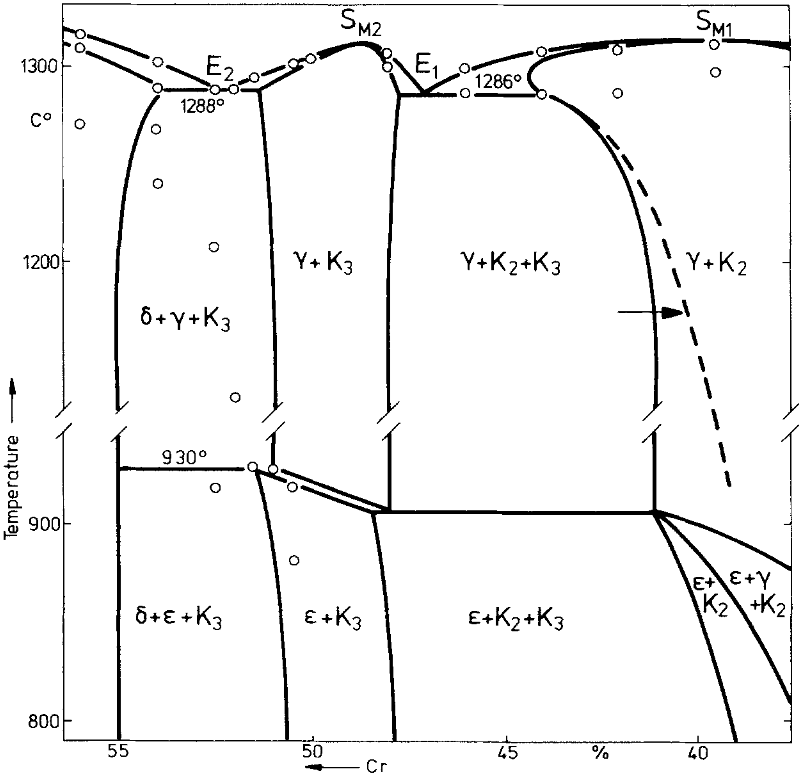

Figure 4 Cut along eutectic trough in the system Co–Cr–C; after Fritscher and Mangers [11].

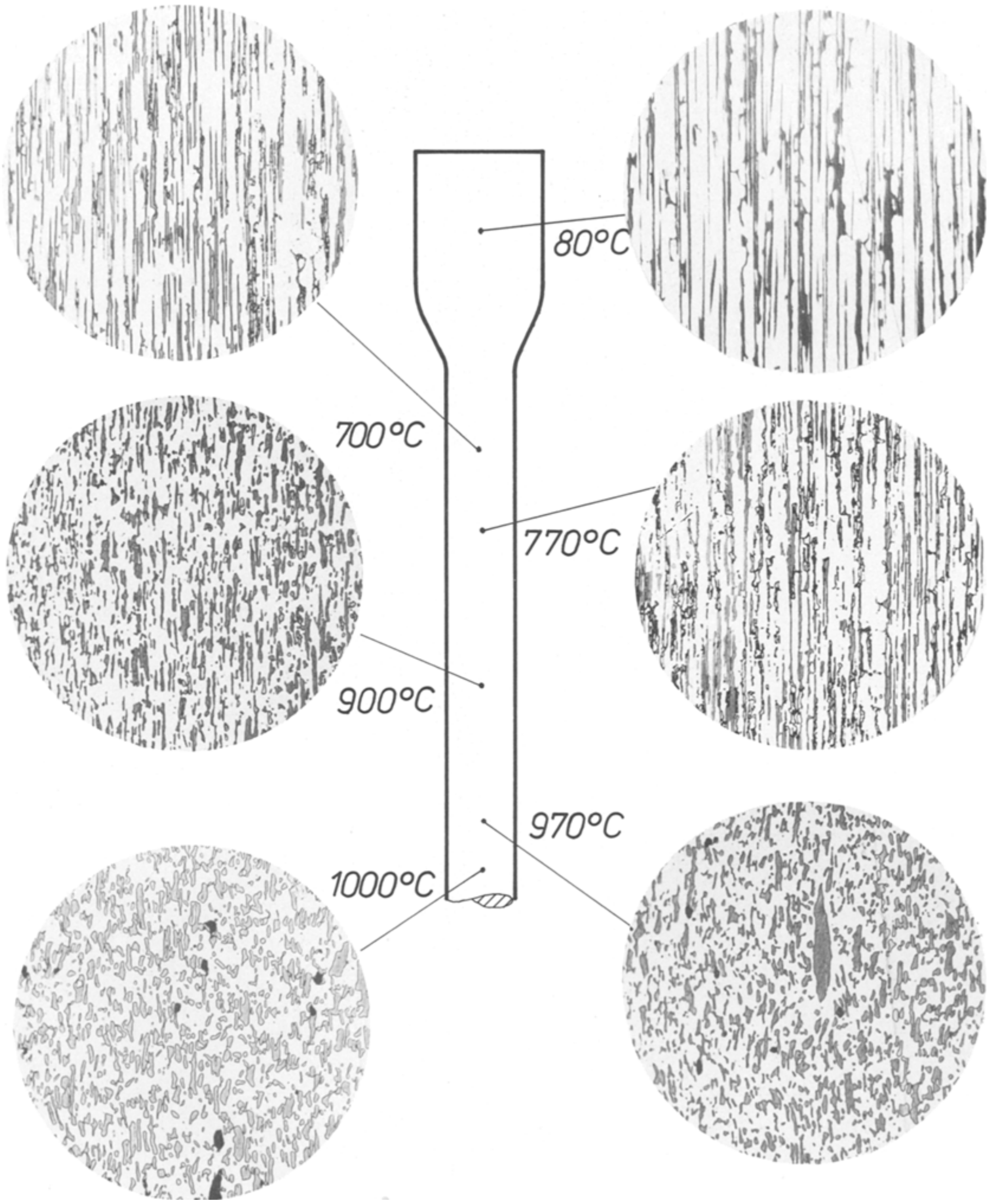

Figure 5 Structure of C73 after 10^4 cycles at different parts of the specimen. Magnification: 210×.

transformation of the reinforced phases were not significantly influenced by the increased quenching rate and compared well to the effects displayed in Fig. 5.

4. Discussion

In the following the effects of irreversible strain will be discussed. To explain irreversible strain effects in this particular eutectic the following possibilities should be weighted against each other: (a) textural phenomena of the anisotropic microstructure; (b) allotropic h c p–f c c transformation of the matrix; (c) two-phase effects.

The anisotropic expansion of any one-phase microstructure is liable to result in geometrical changes if "soft" and "hard" portions of the sample in question are allowed to expand and contract to beyond the proportionality limit

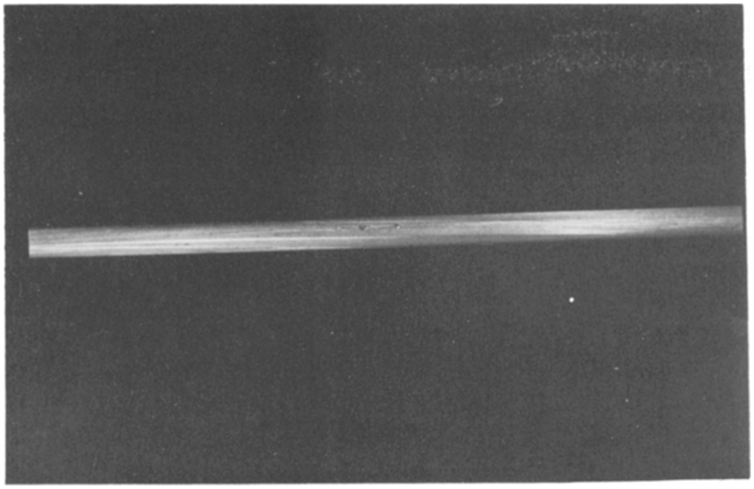

Figure 6 Typical large-grained Co–Cr–Al–C ingot used in measurements.

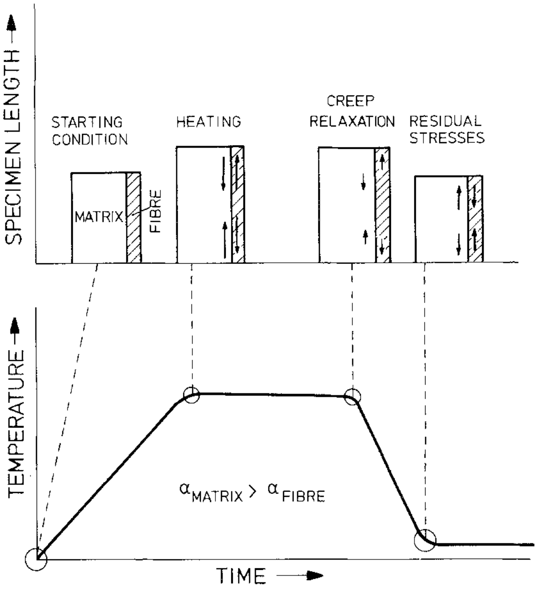

Figure 7 Stresses in a two-phase material under thermal cycling.

relative to each other. Such a model has been proposed by Burke and Turkalo in 1952 [2] ("thermal ratchet"). In the case discussed here, one would have to assume grain boundary ("soft portions") gliding to work against slip in crystals ("hard portions"). Since the sample utilized in the measurements were relatively coarse-grained, Fig. 6, textural phenomena were excluded from further reasoning.

The allotropic transformation of the Co-base matrix, with an hcp–fcc transition temperature of about 950° C (Perry *et al.* [3]) in the basic alloy containing no Al appears to be "smeared out" by Al additions, in particular with respect to a volume change – as our own dilatometric measurements indicate (see also Diderich *et al.* [4]). It has been stated, however, that stress enhances the Co–ϵ–γ–transformation. Therefore, this process may not be completely excluded in the explanation of irreversible strain, especially if considered in connection with two-phase effects to be discussed below.

Air quenching resulted in a permanent sample strain which could not be observed with water quenching. Such irreversible strains may be expected particularly in composites with phases of different thermal expansion characteristics. If the elastic strain due to thermal expansion during the temperature cycle cannot be relieved by creep relaxation, and this resulting stress exceeds the elastic limit, a permanent plastic deformation will remain, see for example [5]. Fig. 7 illustrates the conditions. The arrows indicate the direction and relative amount of strain. The normal condition is thus matrix under tensile stress.

Since water quenching does not result in significant remaining strains (and this may support the theory that allotropic transformations are partially responsible for the observed effects), the strains occurring are apparently being relieved. An explanation by a deformation rate dependence of the proportionality limit appears possible. The following estimates may support this opinion.

For complete creep relaxation at $T_{\max}$ the internal stress on the matrix at temperature $T_{\min}$ may be given by;

$$\sigma_i = E_M(T_{\min}) \cdot \overbrace{(\alpha_M - \alpha_F)}^{\Delta\alpha} \cdot \overbrace{(T_{\max} - T_{\min})}^{\Delta T}, \tag{1}$$

where M denotes the matrix, F denotes the fibre, $T_{\max}$ and $T_{\min}$ are the maximum or minimum

TABLE I Experimental data for the calculation of irreversible sample strains of Co–Cr–Al–C alloy

Parameter	H_2O	Air	Remarks
Cooling rate $\dot{T} = dT/dt$	150 K sec^{-1}	20 K sec^{-1}	Average cooling rate between T_{max} and lowest temperature
	450 K sec^{-1}	97 K sec^{-1}	Initial cooling rate (see Fig. 2)
Proportionality limit of Co–Cr–Al–C alloy $\sigma_{0.2} \simeq \sigma_B$ at 50 to 150° C and $\dot{\epsilon} = 4 \times 10^{-3}$ sec^{-1}	1.5 GPa	1.5 GPa	See [7]
Proportionality limit of the matrix (approximated)	$\rightarrow 0.6\ \sigma_B = 0.9$ GPa (at 50° C)	$\rightarrow 0.5\ \sigma_B = 0.75$ GPa (at 150° C)	*Calculated after Thompson *et al.* [8]
α_M (K^{-1})	14.7×10^{-6}	15.3×10^{-6}	Hildebrandt *et al.* [7]
α_M (K^{-1})	10×10^{-6}	10×10^{-6}	Koss and Copley [9]
E_M (T) (GPa)	E_M(50° C) = 230 GPa	E_M(150° C) = 220 GPa	Koss and Copley [9]* (extrapolated)

* These values are valid for the base material Co–Cr_7C_3 without Al.

cycle temperatures, E is the modulus of elasticity, and α is the thermal expansion coefficient. For plastic deformation not to occur, the following condition applies

$$\sigma_{Mp}(T, \dot{\epsilon}) \geqslant \sigma_i, \qquad (2)$$

where $\dot{\epsilon}$ is the strain rate and p is the proportionality limit.

To calculate the dependence of stress on strain rate ($\dot{\epsilon}$) an equation from the activation theory of dislocation movement is utilized (see for example [6]);

$$\sigma(\dot{\epsilon}_2) = \sigma(\dot{\epsilon}_1)[1 + A \ln(\dot{\epsilon}_2/\dot{\epsilon}_1)]. \qquad (3)$$

The proportionality constant A contains the activation volume. Creep rupture curves [7] deliver a value for A of 0.04. Values necessary to estimate the stresses σ_{Mp} and σ_i are given in Table I for both water and air quenching.

According to Equation 1, the internal stresses are then:

$$\sigma_i = 220(5.3 \times 10^{-1})850 \sim 1 \text{ GPa (air)}$$

and

$$\sigma_i = 230(4.7 \times 10^{-6})950 \sim 1 \text{ GPa (water)}.$$

The deformation rate during quenching is expressed as:

$$\dot{\epsilon}_A = \Delta\alpha\dot{T} \qquad (4)$$

The known matrix strength for the condition of $\dot{\epsilon} = 4 \times 10^{-3}$ sec^{-1} must now be converted to a strength at $\dot{\epsilon}_A$. Equation 3 and Table I yield the following result:

$$\text{air: } \sigma_{Ms}(150° \text{C}, \dot{\epsilon}_A) = 0.75 \times \left[1 + 0.04 \ln\left(\frac{20 \times 4 \times 7 \times 10^{-6}}{4 \times 10^{-3}}\right)\right] = 0.64 \text{ GPa}$$

$$\text{water: } \sigma_{Ms}(50° \text{C}, \dot{\epsilon}_A) = 0.9 \times \left[1 + 0.04 \ln\left(\frac{150 \times 4 \times 7 \times 10^{-6}}{4 \times 10^{-3}}\right)\right] = 0.84 \text{ GPa}$$

Neither of these conditions meets the requirements of Equation 2 since both 0.64 and 0.84 are less than 1.0, but in the case of water quenching plastic deformation is much less than in air quenching, since the elastic limit seems to be about 30% higher.

Assuming partial creep relaxation at T_{max} during one thermal cycle, which is more tenable than complete relaxation, the internal stress σ_i at T_{min} will be lower. If only a factor of 0.7 is involved, Equation 2 can be fulfilled exactly. Thus, within the accuracy of the model, the significantly lower strain for water quenching (1% after 3250 cycles) compared with air quenching (10 to 15%) appears to be not unreasonable.

Acknowledgements

The authors wish to thank Mr A. R. Nicoll and Mr G. Beck for the alloy preparation and experimental work. They are also indebted to Miss B. Herff for much of the metallography. Part of this work was supported by the German Federal Ministry of Research and Technology.

References

1. M. GELL, "Directionally Solidified *In-situ* Composites", edited by E.R. Thompson and P.R. Sahm (AGARD, Washington D.C., 1974) p. 117.
2. J.E. BURKE and A.M. TURKALO, *Trans. Metall. Soc. AIME* **194** (1952) 650.
3. A. J. PERRY, A. R. NICOLL and P. R. SAHM, Brown Boveri, Central Research Laboratory, Heidelberg, Germany (unpublished work).
4. E. DIDERICH, J. M. DRAPIER, D. COUTSOURADIS and E. HABRAKEN, *Cobalt* **S1** (1975) 6.
5. W. EPPRECHT, *Z. Metkde.* **59** (1968) 1.
6. D.L. DAVIDSON, U.S. LINDHOLM and L.M. YEAKLY, *Acta Met.* **14** (1966) 703.
7. U. W. HILDEBRANDT, A. R. NICOLL and P. R. SAHM, Brown Boveri, Central Research Laboratory, Heidelberg, Germany (unpublished work).
8. E.R. THOMPSON, D.A. KOSS and J.C. CHESTNUTT, *Met. Trans.* **1** (1970) 2807.
9. D.A. KOSS and S.M. COPLEY, *ibid* **2** (1971) 1557.
10. P.R. SAHM, M. LORENZ, W. HUGI and V. FRÜHAUF, *ibid* **3** (1972) 1022.
11. K. FRITSCHER and H. MANGERS, Report DFVLR No. IB 012-72/20, Porz-Wahn, Germany (1973).

Received 27 June and accepted 13 September 1977.